# Precision measurement of scattering from three-nucleon short range correlations in Hall A at 1.6< $Q^2$ <1.9 (GeV/c)$^2$

J. Arrington, P. Solvignon
*Argonne National Laboratory, Argonne, IL 60439*

D. Higinbotham, D. Meekins
*Thomas Jefferson National Accelerator Facility, Newport News, VA 23606*

D. B. Day
*University of Virginia, Charlottesville, VA, 22901*

## Abstract

We propose to perform a precision test of scaling in the region dominated by scattering from three-nucleon short range correlations (3N-SRC) in Hall A. If scaling in this region is valid, then one can use the ratio of scattering from heavy nuclei to $^3$He as a measure of the relative contribution of 3N-SRC in heavier nuclei. The kinematics are chosen to access the $x > 2.2$ region using an incident beam energy of 4.137 GeV, and the Hall A left high resolution spectrometer in its standard configuration at two scattering angles of 19° and 20°. In addition to confirming the dominance of 3N-SRC, this measurement will be able to provide a better quantitative extraction of the contribution of 3N-SRC in nuclei, as well as providing more detailed information on the $x$ and $Q^2$ dependence. Four nuclear targets will be used: $^3$He, $^4$He, $^{12}$C and $^{63}$Cu, and the experiment requires two days of beam time.

# 1 Motivations

Recent results from Jefferson Lab Hall B [1] confirmed the scaling behavior of two-nucleon short-range correlations for $Q^2 > 1.4(\mathrm{GeV/c})^2$ with $1.5< x <2.0$ (see Fig. 1).

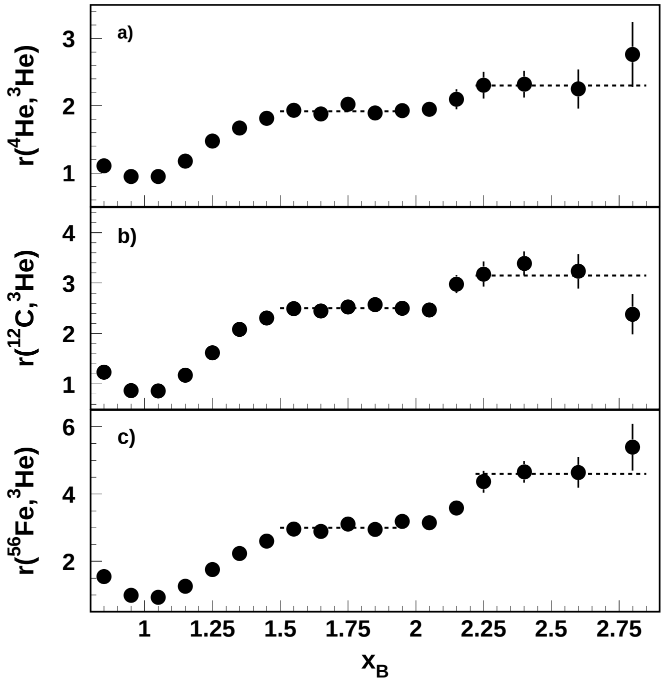

Figure 1: 2N and 3N correlations from recent JLab Hall B data [1]. See text for definition of $r$.

The ratio plotted are defined as follows:

$$r(\mathrm{A}, {}^3\mathrm{He}) = \mathrm{K}_3(\sigma_\mathrm{n}, \sigma_\mathrm{p})\mathrm{R}(\mathrm{A}, {}^3\mathrm{He}) \tag{1}$$

with $K_3(\sigma_n, \sigma_p) = \mathrm{A}(2\sigma_\mathrm{p} + \sigma_\mathrm{n})/3(\mathrm{Z}\sigma_\mathrm{p} + \mathrm{N}\sigma_\mathrm{n})$ and was found [1] equal to 1.14±0.02 for $^4$He and $^{12}$C, and 1.18±0.02 for $^{56}$Fe in the $Q^2$-range between 1.4 and $2.6(\mathrm{GeV/c})^2$ (with and average $Q^2$ value of $1.5–1.6(\mathrm{GeV/c})^2$). In the scaling region, where the scattering from all nuclei is dominated by scattering from 3N-SRC, this ratio is then related to the probability of finding a 3N-SRC in the nucleus, relative to the probability of finding an identical high-momentum configuration in $^3$He, where this is the *only* configuration that can contribute.

An indication of scaling was observed for the first time in the x-region between 2.25 and 2.80 which would correspond to three-nucleon short range correlations. But these data are have significant limitations that make it difficult to make a quantitative extraction of the 3N-SRC probabilities, or even to ensure that the measurement is directly sensitive to the 3N-SRC contributions.

## 2 Details of the previous measurement

The experiment (Ref. 2) assumed that scaling set in for 3N-SRC at the same $Q^2$ as for 2N-SRC. They then observed a scaling region above $x = 2.25$ (Fig. 1) and used the A/$^3$He ratio above $(x, Q^2)$=(2.25,1.4 GeV$^2$) to determine the ratio of 3N-SRC in nuclei. However, there is no guarantee that the scaling will be at the same $Q^2$ for both 2N and 3N-SRC, and in fact the scaling *should* set in at different $(x, Q^2)$ values for different nuclei.

For the Hall B measurement, there is certainly an indication of scaling beginning at $x = 2.25$, but because of both the statistics and the moderate CLAS resolution, it is difficult to determine exactly where the plateau begins. As nearly half of the data is in this lowest $x$ bin, there is some possibility of additional systematic uncertainty if scaling has not fully set in for all of the data.

More importantly, there is some indication that scaling has *not* set in at the $Q^2$ of this measurement, as seen in the $Q^2$-dependence of the 3N-SRC as shown in Fig. 2(b). The quantity $a_3(^{56}\mathrm{Fe}/^3\mathrm{He})$ corresponds to the per-nucleon probability of 3N-SRC in $^{56}$Fe relative to $^3$He and was extracted by fitting or averaging the $x > 2.25$ data. It can be observed that the lowest $Q^2$ point dominates the averaging. Hence a $Q^2$-dependence as well as no $Q^2$-dependence can be deduced depending on which combination of points is used [2]. For example, the average of the three last points gives approximately $a_3(^{56}\mathrm{Fe}/^3\mathrm{He}) \approx 5.8 \pm 0.6$, compared to the lowest $Q^2$ point, which gives $a_3(^{56}\mathrm{Fe}/^3\mathrm{He}) \approx 4.2 \pm 0.2$. So 80–90% of the statistics come from the lowest $Q^2$ bin, which is approximately $2.5\sigma$ from the average of the higher $Q^2$ data. This is not strong enough to conclude that scaling is not valid, but makes it difficult to argue that scaling has been demonstrated at the level necessary for a quantitative extraction of the 3N-SRC probabilities. More precise data, especially at somewhat larger $Q^2$, are needed to precisely determine $a_3(\mathrm{A}/^3\mathrm{He})$ and to clarify its $Q^2$ and $x$ dependence.

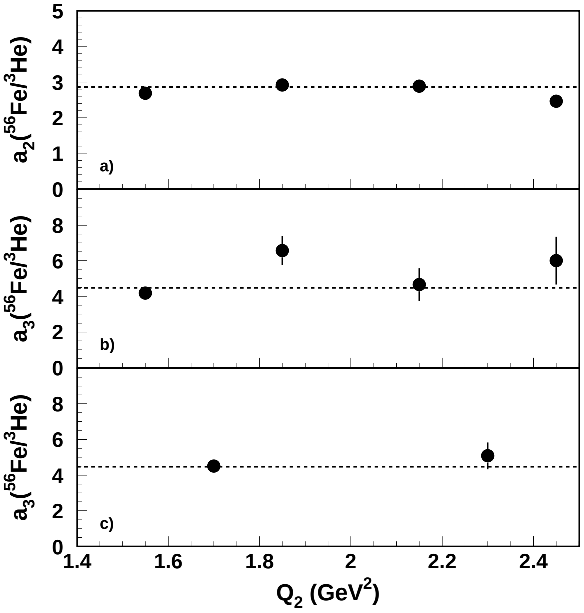

Figure 2: $Q^2$-dependence of 2N and 3N correlations for $^{56}$Fe from recent JLab Hall B data [2]. See text for definition of $a_3(^{56}\mathrm{Fe}/^3\mathrm{He})$.

## 3 The proposed measurement

We propose to perform precision measurements of the inclusive electron scattering cross sections of $^3$He, $^4$He, $^{12}$C and $^{63}$Cu with an incident beam energy of 4.137 GeV and at scattering angles of 19° and 20° focusing on the $x > 2$ region. The corresponding central momenta are 3.717 and 3.687 GeV/c. The $Q^2$ and $x$ ranges covered by these kinematics are summarized in Table 1.

During experiment E04-018, the left HRS will be setup for electron detection, so no particular hardware installation will be required. The beam energy is sufficiently high to make these measurements, but are low enough to detect the electrons in the HRS. The long $^3$He and $^4$He cells are ideal, as they allow for a smaller relative endcap contribution as one approaches $x \to 3$, the kinematic endpoint for $^3$He. The long target allows one to cut away the endcap contribution, or subtract it much more reliably than with the shorter cells. Thus, the conditions during the E04-018 experiment are

| $E$ (GeV) | 4.137 | |
|---|---|---|
| HRS | left | |
| $\theta$ | 19° | 20° |
| $P_0$ (GeV/c) | 3.717 | 3.687 |
| $Q^2$ (GeV/c)$^2$ | 1.63-1.73 | 1.78-1.89 |
| $x$-range | 1.63-2.98 | 1.70-2.98 |

Table 1: Kinematics proposed using only left HRS.

nearly ideal for this test, and thus an extremely useful measurement can be accomplished in less than two days.

### 3.1 Cryotarget: Aluminum window contribution

The $^3$He and $^4$He cryotargets is contained in aluminum cans made from Aluminum 7075-T6 of density of about 2.8g/cm$^3$. The aluminum windows are equivalent to ≈18% of the $^3$He and $^4$He respective thicknesses (Table 2). Because the ratio of the Al to $^3$He cross sections in this region is roughly 3–4 (estimating from Fig. 1, the Al contribution is more than 30% of the total measured cross section on the $^3$He target. We will use software cuts to remove the endcap contributions, and also take data on a empty aluminum can with the same thicknesses to test the efficiency of the cuts, and to subtract any residual endcap contribution. We can also test this by removing the software cuts and subtracting the full endcap contribution.

| Target | $T$(K), $P$(atm), $L$(cm) | Thickness(g/cm$^2$) |
|---|---|---|
| $^3$He | 6.5, 12.0, 20.0 | 0.848 |
| $^4$He | 6.5, 12.0, 20.0 | 1.126 |
| Entrance | N/A, N/A, 0.0279 | 0.078 |
| Exit | N/A, N/A, 0.0277 | 0.078 |
| Wall | N/A, N/A, 0.0311 | 0.087 |

Table 2: Al window contribution. The temperature and pressure of the cryotarget are from [3].

However, an effective way to remove the Al window contribution from the data is to apply a software cut on the target length. This can be precisely done thanks to the high resolution of the Hall A spectrometers. Therefore, in the rate calculations for this proposal, an effective target length of 15cm was used (instead of the physical length of 20cm). We can check how well we can remove the window events as soon as E04-018 starts running.

In both methods, data on a dummy aluminum target will be needed in order to subtract the window contribution or to optimize the software cut on the cryotarget length.

### 3.2 Pion contamination

The expected pion background has been evaluated using experimental data of JLab Experiment E89-008. For an incident energy of 4.045GeV and at a scattering angle of 23°, the $\pi/e$ ratio was found to be approximately 10:1 for a 2% RL carbon target at a momentum setting of 3.76GeV and 4:1 for a 2% RL iron target at 3.60GeV.

The PID performance of Hall A HRS detectors has been shown to be very good in past experiments (see [4], for example) allowing a reduction of the pion background by a factor of about $10^4$, while keeping an electron efficiency better than 99%, when $CO_2$ gas Čerenkov counter and double-layer lead glass calorimeter are associated.

### 3.3 Expected results

To estimate the coverage and the precision of the proposed measurements, a conservative momentum bite of ±3% was used. This is sufficient to fully cover the 3N-SRC region in one setting, although using the full HRS momentum acceptance will improve the coverage in the 2N-SRC region. The data were binned in $x$ with a binsize of 0.1. Respecting the beam current limit allowed on each target (see Table 3), the projected statistical uncertainties were estimated after optimizing the limited time available for the measurements. For the cryotarget, the beam current limitation is due to the coolant restriction.

The rates for $^3$He were evaluated using the XEM cross section model [5] based on y-scaling for the large $x$ region. The XEM model was compared with existing data for $^3$He [6] at lower $Q^2$, closer to the range of the proposed measurements. At these lower $Q^2$ values, the model is in reasonable agreement with the data, but the model seems to underestimate the data by up to a factor of two. Therefore, this model represents a conservative estimate of the cross sections, and our rate estimates could be up to a factor two bigger.

The cross sections for heavier nuclei ($^4$He and carbon) were estimated using the XEM model for $^3$He and the ratio A/$^3$He from the Hall B SRC

| Target | $T$ (K) | $P$ (atm) | length (cm) | RL (g/cm$^2$) | $I^{limit}$ ($\mu$A) |
|---|---|---|---|---|---|
| $^3$He | 6.5 | 12.0 | 20.0 | 0.636 | 60.0 |
| $^4$He | 6.5 | 12.0 | 20.0 | 0.844 | 60.0 |
|  | thickness (cm) |  |  |  |  |
| $^{12}$C | 0.5 |  |  | 1.133 | 100.0 |
| $^{63}$Cu | 0.1 |  |  | 0.896 | 80.0 |

Table 3: Cryo-target characteristics from [3] (top part) and, solid targets and their characteristics asked for this proposal (bottom part).

results. Considering that the scaling factor between the model and Hall B at a given x for the nucleus $A > 3$ is $S_A$, we can write:

$$S_A \cdot r^{model}_{A/3He} = r^{HallB}_{A/3He} \quad \Rightarrow \quad S_A \cdot \sigma^{model}_{A>3} = \sigma^{HallB}_{A>3} \tag{2}$$

The resulting uncertainty on the ratio from the scaled model will be expressed as follows:

$$\Delta r_{A/3He} = r^{HallB}_{A/3He} * \sqrt{\left(\frac{\Delta\sigma^{model}_{A}}{\sqrt{S_A}\cdot\sigma^{model}_{A}}\right)^2 + \left(\frac{\Delta\sigma^{model}_{3He}}{\sigma^{model}_{3He}}\right)^2} \tag{3}$$

For copper, a logarithmic extrapolation with respect to A was done to estimate the values of $a_2(^{63}\mathrm{Cu}/^{3}\mathrm{He})$ and $a_3(^{63}\mathrm{Cu}/^{3}\mathrm{He})$. Then the $^{63}$Cu cross sections from the model were scaled using the same procedure as above.

The $^4$He, carbon and copper target running times were optimized by requiring that the contribution of the relative uncertainty from nucleus A is equal to the $^3$He one in Eq (3), or:

$$\frac{\Delta\sigma_A}{\sqrt{S_A}\cdot\sigma_A} = \frac{\Delta\sigma_{3He}}{\sigma_{3He}} \tag{4}$$

The angular acceptance $\Delta\Omega$ was estimated at 3.2msr and a conservative momentum bite $\Delta P$ of ±3% was chosen. The luminosity $\mathcal{L}_A$ from scattering on a nucleus A can be written as:

$$\mathcal{L}_A = \frac{I}{e}\cdot\rho_A\cdot T_A \tag{5}$$

with the beam current $I$ in Amps, the target density $\rho_A$ in cm$^{-3}$ and the target thickness in cm. The constant $e$ corresponds to the electron charge.

Table 4 gives an estimate of the rates for the two scattering angles considered in Table 1. No prescale will be needed: considering events from the full spectrometer acceptance, the Aluminum window and wall for the cryotarget and the fact that the cross sections might be up to a factor of two larger than estimated by the XEM model, the maximum rate is still less than 1 kHz for all targets and angles.

| Target | $I$ | $\rho_A$ | $T_A$ | $\mathcal{L}_A$ | $\theta = 19°$ | | $\theta = 20°$ | |
|---|---|---|---|---|---|---|---|---|
| | | $\times 10^{21}$ | | $\times 10^{36}$ | $\mathcal{R}_A$ | time | $\mathcal{R}_A$ | time |
| | ($\mu$A) | (cm$^{-3}$) | (cm) | (cm$^{-2}$ s$^{-1}$) | (Hz) | (h) | (Hz) | (h) |
| $^3$He | 60.0 | 8.47 | 15.0 | 47.6 | 19.2 | 8.0 | 8.6 | 10.0 |
| $^4$He | 60.0 | 8.47 | 15.0 | 47.6 | 44.2 | 3.5 | 19.9 | 4.4 |
| $^{12}$C | 100.0 | 95.6 | 0.5 | 29.8 | 104.1 | 1.5 | 46.8 | 1.9 |
| $^{63}$Cu | 80.0 | 84.9 | 0.1 | 4.25 | 92.9 | 1.7 | 42.0 | 2.2 |
| **Total time needed** | | | | | **14.7** | | **18.5** | |

Table 4: Estimated rates and time needed for these proposed measurements. We use the copper solid target instead of iron in order to avoid melting problems.

The projected statistical uncertainties from the run times listed in Table 4 (assuming 100% efficiency) are plotted in Fig. 3. In Fig. 4, we show the uncertainties and $Q^2$-coverage we can achieve in the study of the $Q^2$-dependence of $a_3$(A/$^3$He). The same thing is shown in Fig. 5 for $a_2$(A/$^3$He) but it is not the primary goal of the proposed experiment.

The CLAS measurements had statistical uncertainties of ≈5% and experimental systematic uncertainties of ≈7%. Even with the assumption that scaling was valid for the $(x, Q^2)$ range of their data, their result for the 3N-SRC contribution was dominated by systematic uncertainties. The combination of Coulomb corrections and SRC-motion, which were estimated but *not* applied, along with the experimental systematics due to combining data from different run periods, led to a total uncertainty of ≈25%. We will achieve much better statistics, allowing for a careful examination of the $x$ and $Q^2$ dependence. Because we will take all of the data at one time, with no kinematic changes between targets, the experimental systematics on the measured cross section ratios will be at the 2–3% level or better. In extracting the relative strength of the 3N-SRC configurations, we will apply corrections for Coulomb distortion and center-of-mass motion of the

SRC, which will yield *total* uncertainties on the ratio of 3N-SRC of ∼10%, dominated by the uncertainty in these corrections. Thus, both the direct experimental measurement and the extracted information on 3N-SRCs will be a factor of two better than the published CLAS results.

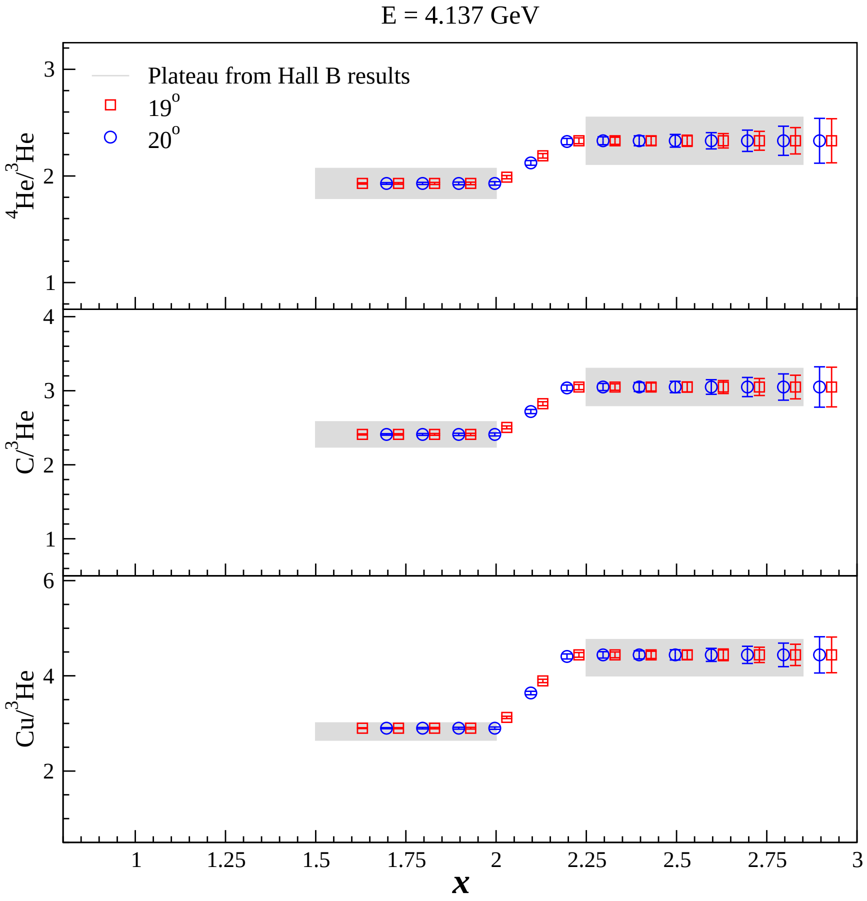

Figure 3: Projected statistical uncertainties for data taken at a beam energy of 4.137GeV and at scattering angles of 19° (red square) and 20° (blue circle) using a copper target. The grey bands represent the resulting fits of the 2N and 3N correlations from recent JLab Hall B data [1].

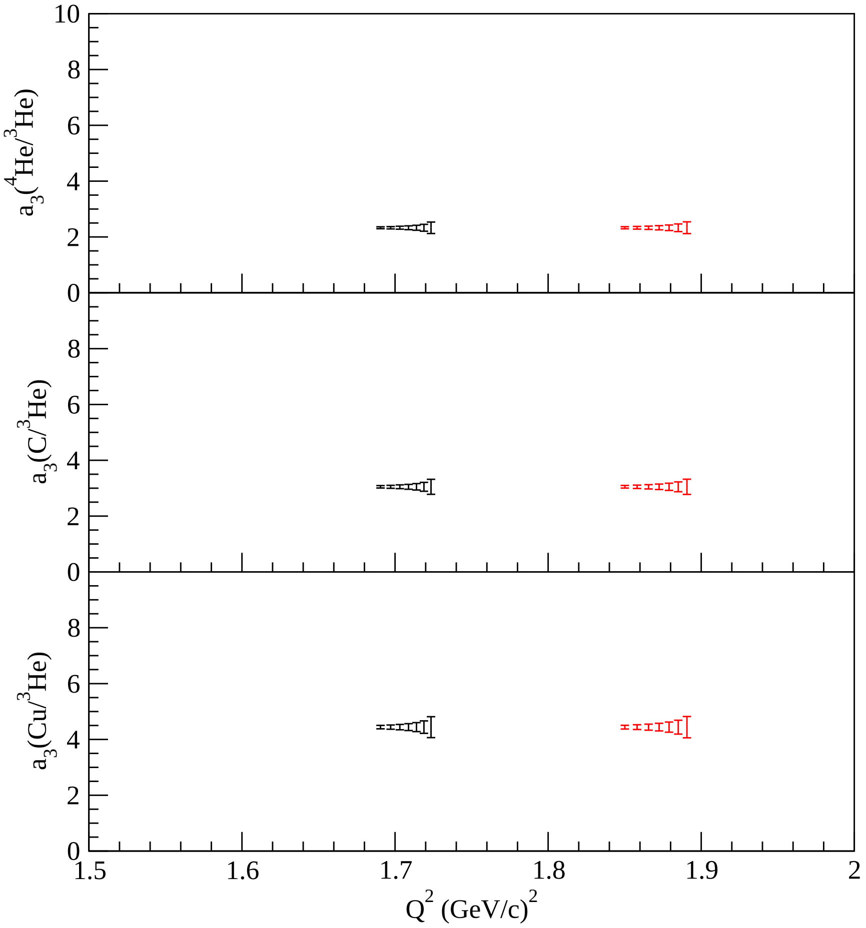

Figure 4: Projected uncertainties on the $Q^2$-dependence of the 3N SRC for data taken at 19° (black) and 20° (red). The y-axis scale was chosen to be directly compare to Fig. 2. The iron projected uncertainties are here as a reference. Note that the CLAS data had an average $Q^2$ of 1.4–1.5 (GeV/c)$^2$

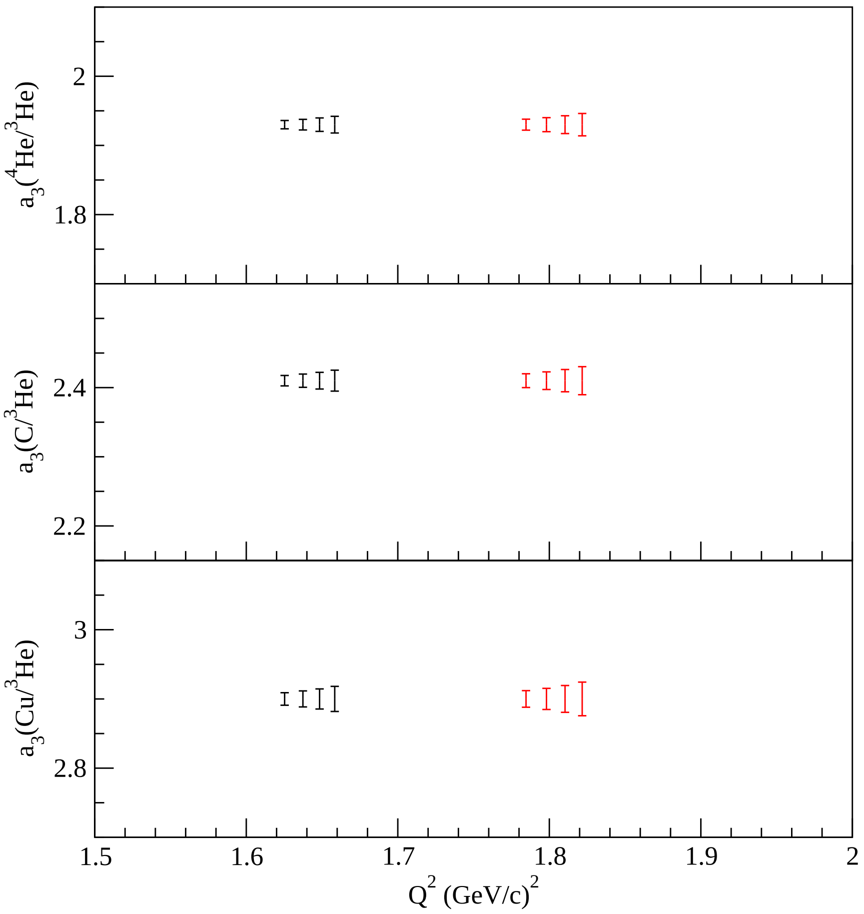

Figure 5: Projected uncertainties on the $Q^2$-dependence of the 2N SRC for data taken at 19° (black) and 20° (red). The iron projected uncertainties are here as a reference.

## 3.4 Overhead time

The total overhead time needed for calibration, background study and configuration changes is now evaluated.

### 3.4.1 Calibration and background study

We will take optics data at both scattering angles. A 30 minute run on carbon foils for each angle will be sufficient.

We will also need to measure the contributions from the aluminum window and wall of the can containing the cryo-target. A 30 minute run will be sufficient for the $^4$He, while the $^3$He runs, where $x \to 3$ is the kinematic limit for scattering from $^3$He, will require runs of 2 hours at both angles. The total time for background studies is 5.5 hours.

### 3.4.2 Configuration changes

The configuration changes necessary to perform the proposed measurements are listed in Table 5.

| Cryo in | $^3$He | | $^4$He | |
|---|---|---|---|---|
| $\theta$ | 20° | 21° | 20° | 21° |
| optics to empty | 10 min | 10 min | 10 min | 10 min |
| empty to cryo | 10 min | 10 min | 10 min | 10 min |
| cryo to $^{12}$C | 10 min | 10 min | | |
| $^{12}$C to $^{63}$Cu | 10 min | 10 min | | |
| $^3$He to $^4$He | 6 hours | | | |
| HRS settings | 30 min | | 30 min | |
| **Total** | **9.0 hours** | | | |

Table 5: Overhead time allocated for configuration changes

The total overhead time allocated for configuration changes is 9.0 hours. We will take $^4$He data at only one angle, to avoid an extra change between the cryotargets. If the run is scheduled during a planned target shift from $^3$He and $^4$He (or vice-versa), the target changeover (assumed to be 6 hours) will not represent additional time.

## 4 Summary

We are requesting 48 hours of beam time, 33 hours for the main data taking, 6 hours for background measurements, and 9 hours overhead, all assuming 100% efficiency (2.5 days, assuming 60% running efficiency). We will need the 20cm $^3$He and $^4$He cryotargets, and empty cell, and a 5mm-Carbon and 1mm-Copper target to perform these measurements. The conditions for the upcoming E04-018 run at 4.137 GeV are ideal for making a very short but high impact measurement testing the assumptions made in the CLAS analysis of 3N-SRC, and making a factor of two improvement on both the direct experimental measurement and the extraction of information on three-nucleon correlations.

## References

[1] K.Sh. Egiyan *et al.*, Phys. Rev. Let. **96**, 082501 (2006)

[2] K.Sh. Egiyan *et al.*, CLAS-NOTE 2005-004, 2005

[3] D. Meekins, *Private communication.*

[4] P. Solvignon, Ph.D thesis, Temple University, 2006

[5] J. Arrington, Ph.D thesis, California Institute of Technology, 1998

[6] O. Benhar, D. Day and I. Sick, nucl-ex/0603032 (2006)